ACS APPLIED MATERIALS & INTERFACES

Research Article

www.acsami.org

On-Surface Formation of Metal Nanowire Transparent Top Electrodes on CdSe Nanowire Array-Based Photoconductive Devices

Daniel Azulai,[†] Uri Givan,[†,‡] Nava Shpaisman,[§] Tatyana Levi Belenkova, Hagit Gilon, Fernando Patolsky,* and Gil Markovich*

School of Chemistry, Raymond and Beverly Sackler Faculty of Exact Sciences, Tel-Aviv University, Tel-Aviv, 69978, Israel

ABSTRACT: A simple wet chemical approach was developed for a unique on-surface synthesis of transparent conductive films consisting of ultrathin gold/silver nanowires directly grown on top of CdSe nanowire array photoconductive devices enclosed in polycarbonate membranes. The metal nanowire film formed an ohmic contact to the semiconductor nanowires without additional treatment. The sheet resistance and transparency of the metal nanowire arrays could be controlled by the number of metal nanowire layers deposited, ranging from ~98−99% transmission through the visible range and several kOhm/sq sheet resistance for a single layer, to 80−85% transmission and ~100 Ohm/sq sheet resistance for 4 layers.

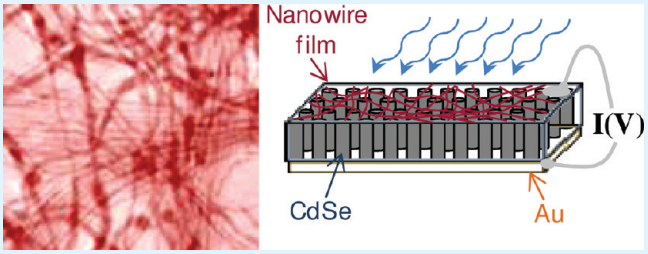

KEYWORDS: *nanowires, transparent conductor, photoconductor, photovoltaic, semiconductor*

INTRODUCTION

The search for new transparent electrode (TE) materials that would replace the transparent conducting oxides (TCOs), e.g. indium tin oxide (ITO), zinc oxide (ZnO), and fluorine doped tin oxide (SnO_2:F), commonly employed for various opto-electronic applications, has been the focus of a series of recent extensive studies.[1]

This quest has been motivated by two main objectives. First, the ever-increasing price of indium and its high vacuum and/or high-temperature deposition process drove the continuous effort to find inexpensive substitutes with similar unique physical properties of high transparency along with low sheet resistivity, whereas the second is the inability of the TCOs family to meet the special requirements of the new generation devices. For instance, TCOs are not fully compatible with novel plastic-based flexible opto-electronic devices. In addition to inexpensive production process, new TE materials have to possess a variety of properties such as flexibility and low temperature implementation, while maintaining their physical properties comparable to those of traditional TCOs.

Recently, a few new promising TE candidates were suggested. The majority of those are based on conducting polymers,[2] in addition to nanoscale materials such as carbon nanotubes,[3−10] graphene flakes,[11−18] hybrid metal−polymers films,[19] nanoscale metallic gratings,[20−23] and random networks of metal nanowires (NWs) made of copper,[24,25] silver,[26−28] and gold−silver.[29] These TEs can potentially meet the new generation device requirements because of their inexpensive deposition processes as well as their flexibility and large-scale implementation. Moreover, their production does not include a high vacuum deposition step, as do traditional TCOs. In addition, the traditional deposition methods are often incompatible with the emerging organic semiconductor-based devices such as light-emitting diodes[30] or transistors[31] due to sensitivity of the organic material to the sputter-coating process. This is basically true when the TC is required as a top electrode in the final phase of the device production. Some of the new TE materials, such as metallic NWs, have an additional key advantage − their solution-based deposition implementation. Solution based deposition methods are typically capable of achieving a uniform coating on top of surfaces with complex shapes and high roughness. The lack of this characteristic in the traditional TCO based TEs, prevented the development of various applications based on NWs or CNTs vertical arrays, such as NW-based photovoltaic cell, which is one of the predominant candidates for future photovoltaic (PV) cells.[32−36]

Azulai et al. have recently demonstrated a new technique for the in situ formation of metal nanowire films on various substrates by drying a thin surfactant film containing metal precursors and ascorbate ions, after initiating metal reduction in the film by seeding with small metal nanoparticles.[29] The present study describes a variation of this method which is a purely self-assembly type process where the nanowire ultrathin film forms spontaneously on dipping the substrate in the growth solution. This new process allows for multilayer nanowire deposition one on top the other and enables tuning of optical transmission vs conductivity of this TE. We also show that such films form good electrical contact to semiconductor substrates on which they are deposited without any special treatments. This is demonstrated by depositing the TE films on a vertical array of CdSe NWs electrochemically grown in a track etched polycarbonate membrane to produce a functional

Received: March 19, 2012
Accepted: May 23, 2012
Published: May 23, 2012

photoconductor with up to 15-fold photocurrent gain and an apparent ohmic contact to the CdSe nanowire elements.

EXPERIMENTAL METHODS

Preparation of the Metal Nanowire Films. The NWs preparation was carried out in a solution of concentrated cetyltrimethylammonium bromide (CTAB) which acted as the templating surfactant. Chloroauric acid and silver nitrate were the Au and Ag precursors, respectively. Sodium ascorbate was used as a mild reducing agent. Mixing together all the components in the order of appearance above, at 35 °C, resulted in the reduction of yellowish Au(III) ions to the colorless Au (I) state, thus forming a $[AuX_2]^-\cdot CTA^+$ complex (X = Cl, Br). Similarly, the Ag^+ ions formed an $[AgX_2]^-\cdot CTA^+$ complex.[43] Further reduction to the metallic state requires additional catalytic metal seed particles.[44] A relatively small amount of sodium borohydride dissolved in water was added to the precursor solution. The sodium borohydride addition resulted in the reduction of up to 0.014% of the metal ions, which then formed small metallic seed particles that catalyzed the reduction of the rest of the metal ions by the ascorbate ions.

Following the formation of the seed particles, about 500 μL of the growth solution were deposited on the front side membrane with the CdSe nanowires on a hot plate heated to 35 °C. The elevated temperature was necessary for the prevention of surfactant precipitation. for ∼15 min. The substrate was then washed by gentle dipping for 1−5 min in an ethanol/water mixture (70/30% by volume). This deposition process was typically repeated 3 times. Prior to nanowire deposition, the membrane edge was protected by coating it with silicon rubber (GE Bayer Silicones RTV 11/DBT) to avoid a short circuit between the two membrane faces.

The deposition processes were repeated over carbon-coated copper grids, 1 cm^2 Si pieces and 2 cm^2 fused silica pieces for TEM, SEM, and optical transmission measurements, respectively.

Metal Nanowire Film Characterizations. The optical transparency of the films was measured against a reference substrate in a fiber-coupled array spectrophotometer (Ocean Optics, S2000) configuration, at a wavelength range of 400−900 nm. Sheet resistance measurements were carried out on the same substrates employing a Fluke true rms multimeter using silver paste at the edges of fused silica substrates for defining the contacts.

CdSe Nanowire Array Preparation. The vertical CdSe NWs array was electrochemically grown, employing a track-etched polycarbonate membrane as a template, as previously described.[41,45] Briefly, polycarbonate membranes with a specified pore diameter of 100 nm and 6 μm thickness (Whatman Inc.) were coated with a 200 nm thick thermally evaporated Au layer. This layer, defining the membrane's back side, served both as a working electrode for the electrochemical deposition process, and as a back contact electrode for the photoconductive device. The membrane was then placed in an electrochemical cell (containing 0.25 M $CdSO_4$, 0.25 M H_2SO_4, and 14 mM SeO_2). The deposition was carried out at room temperature employing a CHI621-A potentiostat (CH Instruments, Austin) with a platinum wire as the counter electrode and an Ag/AgCl (3 M NaCl) reference electrode. During the electrodeposition process, the potential was held at a constant optimized voltage of −0.75 V (versus the Ag/AgCl reference electrode) for 20 min. Once the CdSe NWs were grown, the electrolyte solution was removed and the electrochemical cell was washed with distilled water, the membrane was carefully wiped and washed with water to remove CdSe residue grown on its surface and then dried under a dry N_2 stream.

Characterization of the CdSe NWs. Characterization of the CdSe NWs was performed after dissolving the polycarbonate membrane using methylene chloride in 1.5 mL Eppendorf tubes. The NWs were then precipitated from the solution through 3 min centrifugation at 2500 rpm, and finally washed several times with methylene chloride. The full characterization details can be found elsewhere.[45] Briefly, the CdSe NWs were found to be polycrystalline, with a chemical composition ratio Cd/Se of ca. 1/1.08.

Photoactive Device Characterizations. Photoactive device characterizations were carried out in a two-probe configuration, employing a probe station (Janis, ST-500), with the bias applied between the Au bottom electrode to the TE via silver paste and the probe station tip. The voltage reading was converted to current using a preamplifier (DL 1211) and was collected through a computer-controlled rack-mounted breakout accessory (National Instruments, BNC 2090) and a DAQ card (National Instruments, PCI-MIO-16XE).

RESULTS AND DISCUSSION

Transmission electron microscopy (TEM) images of a typical nanowire film formed by self-assembly on a carbon-coated copper-grid are shown in Figure 1b, c. A single film of this type deposited on glass, SiO_2 or transparent plastic would typically have a sheet resistance on the 1×10^3 Ω/sq scale and net light transmission (relative to the bare substrate) of >98% throughout the visible range.

The high optical transmission, in addition to the good contact between layers, allowed us to perform multiple layer depositions, up to 4 layers, where after 3 deposition cycles the sheet resistance decreased to ∼100 Ω/sq with an optical transmission of ∼88% at a wavelength of 600 nm.

Figure 1a shows a scanning electron microscope (SEM) image of a focused ion beam (FIB) cut of a nanowire film deposited by the self-assembly process, excess solution removed, and the remaining solution film dried without washing. This cut shows that a ∼10 nm thick nanowire film is located primarily at the interface between the substrate and the surfactant film with the occasional formation of an additional layer of wires within the surfactant film, which is ∼100 nm thick. Thus, it seems that the particular (tubular) surfactant phase which forms the template for nanowire formation is almost unique to the interface. Such effects of interface sensitive order were also observed in thin films of mesoporous materials using the same surfactant.[37]

Figure 1d presents the level of our current understanding of the mechanism leading to nanowire formation; as the substrate is dipped into the growth solution, after triggering the formation of small metal seed particles in solution, the surfactant molecules quickly accumulate at the substrate-solution interface. In addition, the seed nanoparticles, coated with a surfactant bilayer, also adsorb to this interface and apparently induce the formation of elongated vesicular structures which connect between several seed particles to form long nanotubules filled with solution. These nanotubules contain the ascorbate ions, which catalytically reduce gold and silver ions complexed with the surfactant at the surface of the seed particles and eventually lead to continuous metal nanowires. The ascorbate served as a mild reducing agent. In the presence of gold seeds the chemical potential of the system decreased to enable reduction of the gold and silver ions at the particle surface. This self- assembly process was performed by dipping the substrate in the growth solution after triggering seed formation for ∼15−20 min, removing the substrate without drying and dipping immediately in a solvent to remove excess surfactant, This process was typically repeated several times in order to achieve the required sheet resistance.

Figure 2 displays the evolution of the resulting nanowire film along the sequential deposition of 3 layers of nanowires, observed both by TEM and SEM. The first layer the nanowire network seems to be a random mesh primarily consisting of bundles of 2−3 nm diameter Au−Ag NWs, entwined into 50−100 nm wide bundles together with a small amount of thicker

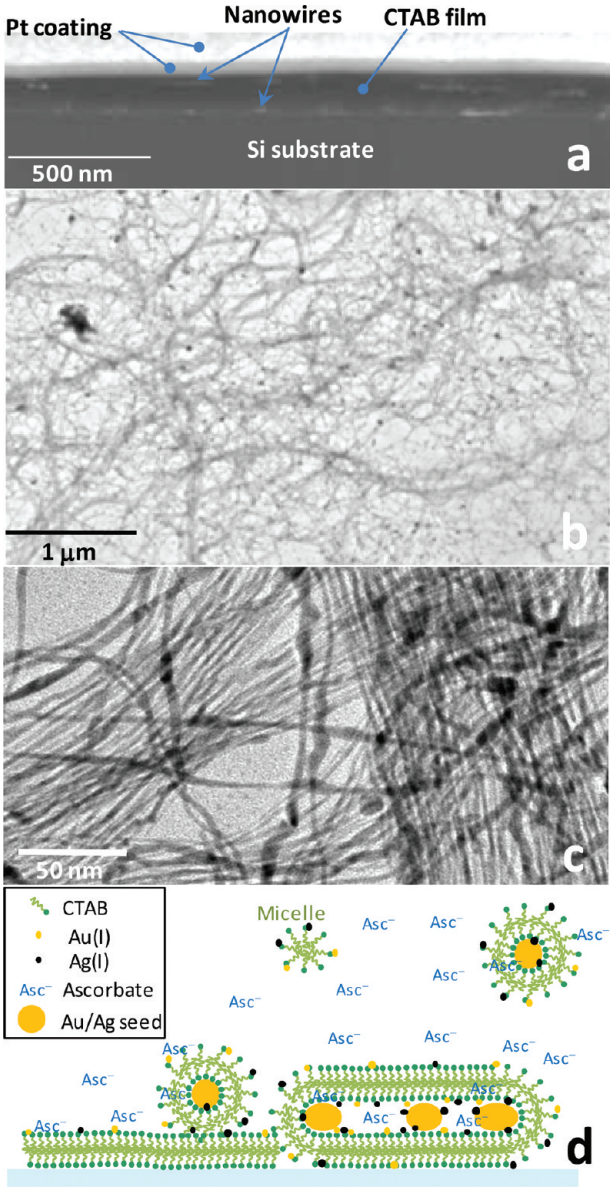

Figure 1. (a) SEM cross-sectional image of a nanowire film deposited on a Si substrate without washing the excess CTAB, which was cut by FIB after deposition of a Pt film on top. (b) TEM image of a similar film deposited on a carbon-coated copper grid and (c) a higher-magnification TEM image of the same film. (d) Scheme of the early stages of nanowire formation. Addition of a small quantity of a strong reducing agent, such as sodium borohydride, initially reduces a small part of the metal ions to form seed particles. The seed particles are coated by a surfactant bilayer and when adsorbed with excess surfactant to the solution–substrate interface fuse into larger tubular-vesicular structures. Then, additional metal ions complexed with the CTAB are catalytically reduced within these structures by ascorbate anions available in large excess.

~20 nm single nanowires. Energy dispersive spectroscopy (EDS) measurements of many bundle segments, by TEM, yielded metal atomic ratios in the range of 75% ± 5% Au to 25% ± 5% Ag, without an observable change on additional layer deposition.

Figure 3 shows the optical transmission spectra and the corresponding sheet resistance of the Au–Ag NWs random network after 1–4 layers deposition steps. A single deposited layer has a net transmission of ~99% at 600 nm, and a sheet

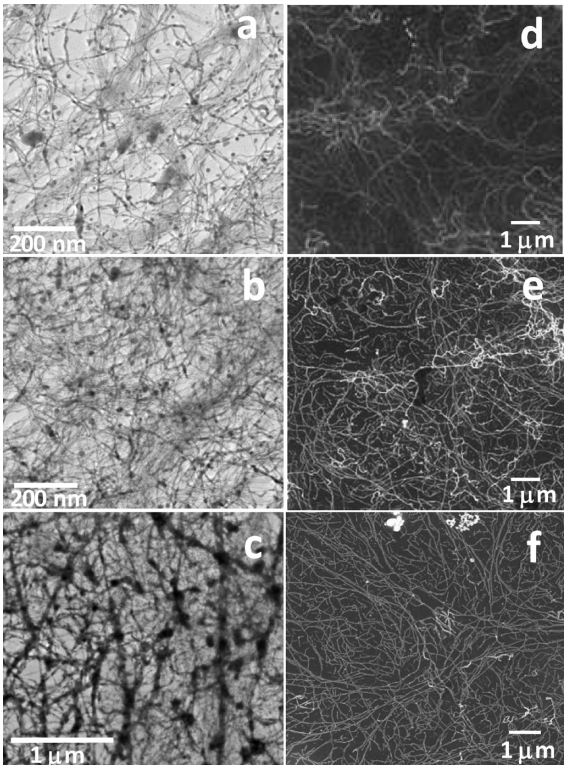

Figure 2. TEM images of (a) a single layer, (b) two layers, and (c) three layers of nanowire films deposited on carbon-coated copper grids, and SEM images of (d) single, (e) two, and (f) three layers of such film deposited on silicon substrates.

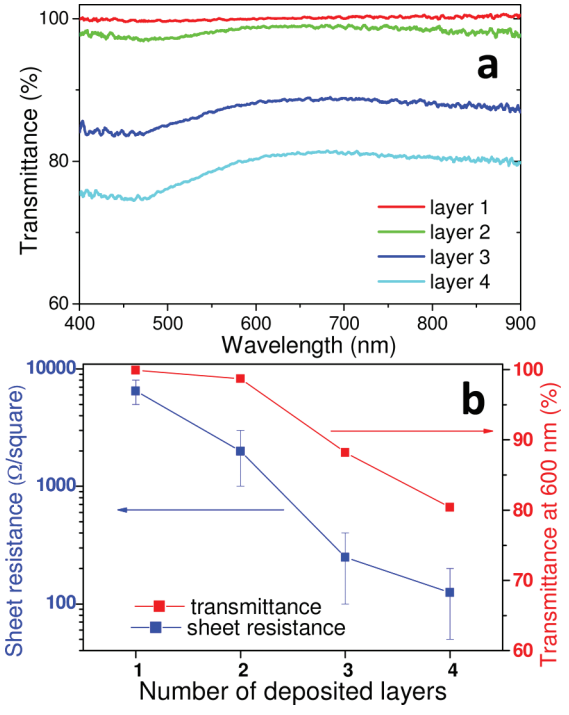

Figure 3. (a) Optical transmission curves for the deposition of four successive layers of Au–Ag nanowires deposited on fused silica. (b) The changes in the optical transmission and sheet resistance with the number of deposited successive layers.

resistance of 5–8 kΩ/Sq. Deposition of a second layer reduced the sheet resistance to 1–3 kΩ/Sq and the resultant

dx.doi.org/10.1021/am3004895 | ACS Appl. Mater. Interfaces 2012, 4, 3157–3162

transmission to 97−98%. Deposition of a third layer further reduced both the sheet resistance and the transmission of the nanowire film to typical values of 100−400 Ω/Sq and 88% (at 600 nm), respectively. The same process was repeated on various substrates, such as silicon, quartz, and polyethylene terphtalate (PET), with up to 5% variation of the measured optical transparency.

TEM and SEM images displayed in Figure 2 can shed light on the relation between the physical properties of the films and the structural evolution of the films with successive deposition steps. The deposition of successive layers resulted in the addition of new nanowire bundles as well as thickening of predeposited wires, which caused the suppression of transmission. This effect is accompanied by a parallel reduction of the sheet resistivity due to the formation of a denser network possessing an increased number of percolating pathways and is, therefore, characterized by a higher electrical homogeneity. In that manner, control of the trade-off between electrical and optical properties is attained. This fact facilitates the tailoring of the TE properties to the desired application.

The extensive ongoing effort to produce vertical semiconductor NW array-based devices such as PV cells[32,33] has influenced our choice to utilize the Au−Ag NWs random network as TEs on top of such a vertical NWs array. Vertical arrays of CdSe NWs were chosen because they were already tested as candidates for photodetectors due to their notable photo gain.[38−41]

Characterization of the CdSe NWs, electrochemically grown in the polycarbonate membranes,[41] was performed by dissolving the polycarbonate template using methylene chloride. Electron microscopy and EDS measurements performed showed that the resulting CdSe NWs were polycrystalline, with a chemical composition ratio Cd/Se of ca. 1/1.08.

The Au−Ag nanowire film deposited on top of the membrane filled with CdSe NWs was confined to the center of the membrane by a ring of PDMS, protecting the edges from deposition of nanowires that might short-circuit to the bottom gold electrode.

A representative SEM image of the surface of the resulting device (Figure 4) shows a random network of Au−Ag NW bundles covering the membrane surface, enabling electric contact with nearly each CdSe NW and a percolating pathway across the device. Some metallic aggregates adsorbed to the metallic bundles and unfilled pores were observed as well.

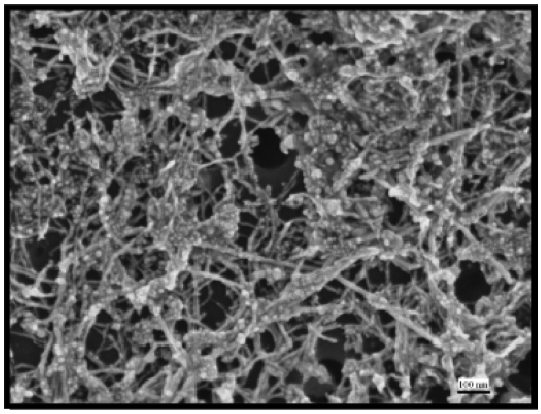

Figure 4. SEM image of the nanowires deposited on top of the polycarbonate membrane filled with CdSe nanowires.

I−*V* measurements were carried out in a two-probe configuration, employing a probe station, with the bias applied between the Au bottom electrode to the TE via silver paste and the probe station tip. Figure 5 presents the *I*−*V* characteristics

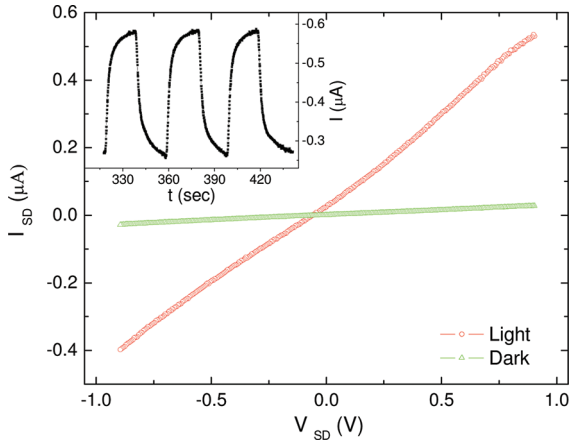

Figure 5. Current vs voltage curves of the CdSe NW-based membrane device, with and without illumination. Inset: Current changes in the device with alternating on−off light cycles.

of the above-mentioned device measured both in dark and under microscope objective white light illumination. A device resistance of ca. 3×10^7 Ω can be calculated from the dark currents under ±1 V. The curve under white-light illumination reveals higher current values throughout the scan from 1 V to −1 V, implying a decrease of device resistivity by a factor of ca. 15, which was observed in both the positive and negative branches of the I−V curve. This behavior is consistent with light-induced increase of free charge carriers' density due to direct band gap excitations, with deep-trap and surface states determining the upper limit of the photoexcitation gain. It is likely that the grain boundaries between nanocrystals in the polycrystalline CdSe NWs contribute substantially to this trapping phenomenon. Similar photoeffects were observed for a variety of CdSe NWs diameters and for Ni upper and bottom contacts as well.[41]

Notable photoconductivity is observed in the inset of Figure 5, representing the effect of switching the light on and off, at 30 s intervals, while maintaining a constant bias of 0.5 V between the bottom contact and the probe station tip.

Response or recovery time of CdSe based opto-electronic devices' photogain (NWs, nanorods and thin films) are usually in the order of microseconds up to milliseconds.[42] The increase in response time from the μs regime to the ms regime is usually attributed to reduction of recombination centers at the NWs surface. Although relatively fast response times (on the order of microseconds) were observed in air environment for both CdSe NWs and for CdSe NRs, a substantial increase to the ms regime took place after coating the CdSe NRs with SiO layer.[46,47] Longer response times, on the order of seconds, were observed with increase of grain size.[47] We believe that the observed long (tens of seconds) response times might be attributed to: (1) reduced recombination centers of the CdSe NWs which are embedded in the polycarbonate membrane with both sides blocked by the electrodes (Au and AuAgNWs as the bottom and upper electrodes, respectively). (2) The device poor

thermal conductivity causing slow thermal processes (heating and cooling). Forced convection by cooling with dry N_2 flow during exposure did show response time reduction. In the present case, the embedded CdSe NWs are less sensitive to the environment and therefore the influence of chemisorption can be ruled out.[48]

An important finding resulting from device measurements is the ohmic behavior of the $I-V$ curves. This indicates that the metal nanowire TE film was able to form a good contact to the underlying CdSe NW elements, in spite of the concentrated CTAB surfactant environment used for this deposition. This is in agreement with the SEM image of the FIB cut shown in Figure 1a, indicating that the nanowire film is located precisely at the interface, probably exposing part of the metal toward the substrate.

CONCLUSION

This work has demonstrated a simple solution-based deposition approach able to easily form a metal NW-based top transparent contact to a photoconductive device, showing ohmic current/voltage characteristics. The sheet resistance and optical transmission of the film could be controlled by changing the number of deposited nanowire layers.

In general, an important aspect of the deposition of the TE film is that it does not require any thermal treatment that may harm the underlaying active layer of the device. This is particularly important in devices consisting of organic materials.

The problem of deposition of top contacts on various types of organic and inorganic semiconductor films is still not well resolved using existing technologies and such a simple solution-based deposition approach may offer an advantage over existing methods in its wide applicability to surfaces of various materials and complex morphologies.

Another important aspect is the flexibility of the resulting contact film (see ref 29). The CdSe NWs-filled PC membrane is a highly flexible substrate and the conductivity of the metal Au–Ag nanowire top contact did not seem to be affected by membrane curvature. This flexibility is an inherent property of such ultrathin nanowire films.

AUTHOR INFORMATION

Corresponding Author

*E-mail: fernando@post.tau.ac.il (F.P.); gilmar@post.tau.ac.il (G.M.).

Present Addresses

[‡]Max Planck Institute for Microstructure Physics, Halle, Germany

[§]Rutgers University, New Jersey Center for Biomaterials, Rutgers, The State University of New Jersey, New Brunswick, NJ 08854–8087, United States

Author Contributions

[†]These authors contributed equally to this work.

Notes

The authors declare no competing financial interest.

ACKNOWLEDGMENTS

The authors are grateful to Denis Glozman for his help with SEM imaging. This work was supported by a Magneton grant from the Israeli ministry of industry, trade and labor in collaboration with PV Nanocell Ltd.

REFERENCES

(1) Kumar, A.; Zhou, C. *ACS Nano* **2010**, *4*, 11–4.
(2) Kim, Y. H.; Sachse, C.; Machala, M. L.; May, C.; Müller-Meskamp, L.; Leo, K. *Adv. Funct. Mater.* **2011**, *21*, 1076–1081.
(3) Fraser, I. S.; Motta, M. S.; Schmidt, R. K.; Windle, A. H. *Sci. Tech. Adv. Mater.* **2010**, *11*, 045004.
(4) Geng, H.-Z.; Kim, K. K.; So, K. P.; Lee, Y. S.; Chang, Y.; Lee, Y. H. *J. Am. Chem. Soc.* **2007**, *129*, 7758–9.
(5) Saran, N.; Parikh, K.; Suh, D.-S.; Muñoz, E.; Kolla, H.; Manohar, S. K. *J. Am. Chem. Soc.* **2004**, *126*, 4462–3.
(6) Zhang, M.; Fang, S.; Zakhidov, A. A; Lee, S. B.; Aliev, A. E.; Williams, C. D.; Atkinson, K. R.; Baughman, R. H. *Science* **2005**, *309*, 1215–9.
(7) Wu, Z.; Chen, Z.; Du, X.; Logan, J. M.; Sippel, J.; Nikolou, M.; Kamaras, K.; Reynolds, J. R.; Tanner, D. B.; Hebard, A. F.; Rinzler, A. G. *Science* **2004**, *305*, 1273–6.
(8) Zhang, D.; Ryu, K.; Liu, X.; Polikarpov, E.; Ly, J.; Tompson, M. E.; Zhou, C. *Nano Lett.* **2006**, *6*, 1880–6.
(9) Jo, J. W.; Jung, J. W.; Lee, J. U.; Jo, W. H. *ACS Nano* **2010**, *4*, 5382–8.
(10) Wakamatsu, N.; Takamori, H.; Fujigaya, T.; Nakashima, N. *Adv. Funcl Mater.* **2009**, *19*, 311–316.
(11) Kim, W. S.; Kim, Y. I.; Kim, H. J.; Hwanag, J. Y.; Moon, S. Y.; Park, N.-H.; Shim, K. B.; Kim, H. W.; Ham, H.; Huh, H. *J. Mater.Chem.* **2011**, *21*, 15655.
(12) Tien, H.-W.; Huang, Y.-L.; Yang, S.-Y.; Hsiao, S.-T.; Wang, J.-Y.; Ma, C.-C. M. *J. Mater. Chem.* **2011**, *21*, 14876.
(13) Eda, G.; Fanchini, G.; Chhowalla, M. *Nat. Nanotechnol.* **2008**, *3*, 270–4.
(14) Bae, S.; Kim, H.; Lee, Y.; Xu, X.; Park, J.-S.; Zheng, Y.; Balakrishnan, J.; Lei, T.; Kim, H. R.; Song, Y. I.; Kim, Y.-J.; Kim, K. S.; Ozyilmaz, B.; Ahn, J.-H.; Hong, B. H.; Iijima, S. *Nat. Nanotechnol.* **2010**, *5*, 574–8.
(15) Wang, X.; Zhi, L.; Müllen, K. *Nano Lett.* **2008**, *8*, 323–7.
(16) Kim, K. S.; Zhao, Y.; Jang, H.; Lee, S. Y.; Kim, J. M.; Kim, K. S.; Ahn, J.-H.; Kim, P.; Choi, J.-Y.; Hong, B. H. *Nature* **2009**, *457*, 706–10.
(17) Wang, S. J.; Geng, Y.; Zheng, Q.; Kim, J.-K. *Carbon* **2010**, *48*, 1815–1823.
(18) Li, X.; Zhu, Y.; Cai, W.; Borysiak, M.; Han, B.; Chen, D.; Piner, R. D.; Colombo, L.; Ruoff, R. S. *Nano Lett.* **2009**, *9*, 4359–63.
(19) Zeng, X.-Y.; Zhang, Q.-K.; Yu, R.-M.; Lu, C.-Z. *Adv. Mater.* **2010**, *22*, 4484–8.
(20) Kang, M.-G.; Guo, L. J. *Adv. Mater.* **2007**, *19*, 1391–1396.
(21) Tvingstedt, K.; Inganäs, O. *Adv. Mater.* **2007**, *19*, 2893–2897.
(22) Ahn, B. Y.; Lorang, D. J.; Lewis, J. A. *Nanoscale* **2011**, *3*, 2700–2.
(23) Layani, M.; Magdassi, S. *J. Mater. Chem.* **2011**, *21*, 15378.
(24) Rathmell, A. R.; Bergin, S. M.; Hua, Y.-L.; Li, Z.-Y.; Wiley, B. J. *Adv. Mater.* **2010**, *22*, 3558–63.
(25) Rathmell, A. R.; Wiley, B. J. *Adv. Mater.* **2011**, *23*, 4798–4803.
(26) Hu, L.; Kim, H. S.; Lee, J.-Y.; Peumans, P.; Cui, Y. *ACS nano* **2010**, *4*, 2955–63.
(27) Lee, J.-Y.; Connor, S. T.; Cui, Y.; Peumans, P. *Nano Lett.* **2008**, *8*, 689–92.
(28) De, S.; Higgins, T. M.; Lyons, P. E.; Doherty, E. M.; Nirmalraj, P. N.; Blau, W. J.; Boland, J. J.; Coleman, J. N. *ACS Nano* **2009**, *3*, 1767–74.
(29) Azulai, D.; Belenkova, T.; Gilon, H.; Barkay, Z.; Markovich, G. *Nano Lett.* **2009**, *9*, 4246–9.
(30) Burroughes, J. H.; Bradley, D. D. C.; Brown, A. R.; Marks, R. N.; Mackay, K.; Friend, R. H.; Burns, P. L.; Holmes, A. B. *Nature* **1990**, *347*, 539–541.
(31) Mentovich, E. D.; Belgorodsky, B.; Kalifa, I.; Richter, S. *Adv. Mater.* **2010**, *22*, 2182–6.
(32) Garnett, E.; Yang, P. *Nano Lett.* **2010**, *10*, 1082–7.
(33) Kelzenberg, M. D.; Boettcher, S. W.; Petykiewicz, J. a; Turner-Evans, D. B.; Putnam, M. C.; Warren, E. L.; Spurgeon, J. M.; Briggs, R. M.; Lewis, N. S.; Atwater, H. A. *Nat. Mater.* **2010**, *9*, 239–44.

(34) Kendrick, C. E.; Yoon, H. P.; Yuwen, Y.; Barber, G. D.; Shen, H.; Mallouk, T. E.; Dickey, E. C.; Mayer, T. S.; Redwing, J. M. *Appl. Phys. Lett.* **2010**, *97*, 143108.
(35) Tian, B.; Zheng, X.; Kempa, T. J.; Fang, Y.; Yu, N.; Yu, G.; Huang, J.; Lieber, C. M. *Nature* **2007**, *449*, 885−9.
(36) Kanungo, P. D.; Kögler, R.; Werner, P.; Gösele, U.; Skorupa, W. *Nanoscale Res. Lett.* **2010**, *5*, 243−246.
(37) Lu, Y.; et al. *Nature* **1997**, *389*, 364−368.
(38) Robel, I.; Subramanian, V.; Kuno, M.; Kamat, P. V. *J. Am. Chem. Soc.* **2006**, *128*, 2385−93.
(39) Fan, Z.; Ho, J. C.; Jacobson, Z. A; Razavi, H.; Javey, A. *Proc. Natl. Acad. Sci. U.S.A.* **2008**, *105*, 11066−70.
(40) Jiang, Y.; Zhang, W. J.; Jie, J. S.; Meng, X. M.; Fan, X.; Lee, S.-T. *Adv. Funct. Mater.* **2007**, *17*, 1795−1800.
(41) Shpaisman, N.; Givan, U.; Patolsky, F. *ACS Nano* **2010**, *4*, 1901−6.
(42) Kung, S.-C.; van der Veer, W. E.; Yang, F.; Donavan, K. C.; Penner, R. M. *Nano Lett.* **2010**, *10*, 1481−5.
(43) Hubert, F.; Testard, F.; Spalla, O. *Langmuir* **2008**, *24*, 9219−22.
(44) Pérez-Juste, J.; Liz-Marzán, L. M.; Carnie, S.; Chan, D. Y. C.; Mulvaney, P. *Adv. Funct. Mater* **2004**, *14*, 571−579.
(45) Reddy, N. K.; Devika, M.; Shpaisman, N.; Ben-Ishai, M.; Patolsky, F. *J. Mater. Chem.* **2011**, *21*, 3858−3864.
(46) Jiang, Y.; Zhang, W. J.; Jie, J. S.; Meng, X. M.; Fan, X.; Lee, S. T. *Adv. Funct. Mater.* **2007**, *17*, 1795.
(47) Kung, S. C.; Xing, W.; van der Veer, W. E.; Yang, F.; Donavan, K. C.; Cheng, M.; Hemminger, J. C.; Penner, R. M. *ACS Nano* **2011**, *5*, 7627.
(48) Kind, H.; Yan, H.; Messer, B.; Law, M.; Yang, P. *Adv. Mater.* **2002**, *14*, 158.